DISCLAIMER

This report was prepared as an account of work sponsored by an agency of the United States Government. Neither the United States Government nor any agency thereof, nor any of their employees, makes any warranty, express or implied, or assumes any legal liability or responsibility for the accuracy, completeness, or usefulness of any information, apparatus, product, or process disclosed, or represents that its use would not infringe privately owned rights. Reference herein to any specific commercial product, process, or service by trade name, trademark, manufacturer, or otherwise does not necessarily constitute or imply its endorsement, recommendation, or favoring by the United States Government or any agency thereof. The views and opinions of authors expressed herein do not necessarily state or reflect those of the United States Government or any agency thereof. Reference herein to any social initiative (including but not limited to Diversity, Equity, and Inclusion (DEI); Community Benefits Plans (CBP); Justice 40; etc.) is made by the Author independent of any current requirement by the United States Government and does not constitute or imply endorsement, recommendation, or support by the United States Government or any agency thereof.

ORNL/TM-2026/4447

Digital Twin User Guide for Chelan County Public Utility District

Sunil Subedi
Hong Wang
Wenbo Jia
Zhun Yin
Scott Warnick

Approved for public release.
Distribution is unlimited.

February 2026

OAK RIDGE National Laboratory

ORNL IS MANAGED BY UT-BATTELLE LLC FOR THE US DEPARTMENT OF ENERGY

DOCUMENT AVAILABILITY

Online Access: US Department of Energy (DOE) reports produced after 1991 and a growing number of pre-1991 documents are available free via https://www.osti.gov/.
The public may also search the National Technical Information Service's National Technical Reports Library (NTRL) for reports not available in digital format.
DOE and DOE contractors should contact DOE's Office of Scientific and Technical Information (OSTI) for reports not currently available in digital format:

US Department of Energy
Office of Scientific and Technical Information
PO Box 62
Oak Ridge, TN 37831-0062
Telephone: (865) 576-8401
Fax: (865) 576-5728
Email: reports@osti.gov
Website: https://www.osti.gov/

This report was prepared as an account of work sponsored by an agency of the United States Government. Neither the United States Government nor any agency thereof, nor any of their employees, makes any warranty, express or implied, or assumes any legal liability or responsibility for the accuracy, completeness, or usefulness of any information, apparatus, product, or process disclosed, or represents that its use would not infringe privately owned rights. Reference herein to any specific commercial product, process, or service by trade name, trademark, manufacturer, or otherwise, does not necessarily constitute or imply its endorsement, recommendation, or favoring by the United States Government or any agency thereof. The views and opinions of authors expressed herein do not necessarily state or reflect those of the United States Government or any agency thereof.

ORNL/TM-2026/4447

Electrification and Energy Infrastructures Division
Buildings and Transportation Science Division

DIGITAL TWIN USER GUIDE FOR CHELAN COUNTY PUBLIC UTILITY DISTRICT

Sunil Subedi
Hong Wang
Wenbo Jia
Zhun Yin
Scott Warnick

February 2026

Prepared by
OAK RIDGE NATIONAL LABORATORY
Oak Ridge, TN 37831
managed by
UT-BATTELLE LLC
for the
US DEPARTMENT OF ENERGY
under contract DE-AC05-00OR22725

CONTENTS

LIST OF FIGURES

LIST OF TABLES

LIST OF ABBREVIATIONS

u	Guided vane opening (time-variant)
v	Excitation control input for generator
AC	Alternating current
AVR	Automatic voltage regulator
DC	Direct current
DT	Digital twin
EMF	Electromotive force
PID	Proportional–Integral–Derivative
PIDD	Proportional–Integral–Double–Derivative
PLC	Programmable logic controller

ABSTRACT

This user manual offers a comprehensive guide for developing a Digital twin (DT) of a Kaplan turbine at Chelan County Public Utility District (Chelan PUD) using neural networks. As variable renewable generation expands, hydropower units must operate with optimal efficiency and stability. For Kaplan machines, this flexibility is achieved through coordinated control of guide vane (wicket gates) opening and runner blade pitch, which amplifies the plant's inherent nonlinear behavior and challenges traditional physics-only modeling. The efficiency of the Kaplan turbine varies with different combinations of the guide vans (wicket gate) opening and the blade angle. Each guide van opening and blade angle has a corresponding highest efficiency point, forming a cam relationship that represents the optimal combination.The discharge of a hydraulic turbine is controlled by the opening angle of the guide vans. Therefore, for each value of head, there is a certain guide van opening and blade angle that corresponds to the highest efficiency. For a given head, different combinations of the guide van opening and blade angle have different efficiencies. Therefore, coordinate cam curves are used to describe the relationship between the wicket gate opening and blade angle with different water head.

To address these challenges, the manual details a data-driven modeling and learning workflow centered on structured neural networks. The approach is designed to forecast critical operational variables—discharge flow, net head, penstock (or scroll-case) pressure, and generator electrical outputs—by leveraging real-time inputs such as the generator power control setpoint, exciter field current and field voltage, together with hydromechanical commands (e.g., gate position and, when available, runner blade-pitch angle). The neural models are trained and validated on operational data from a Kaplan unit operated by Chelan PUD, demonstrating that the structured NN architecture can learn the coupled gate–blade–electrical dynamics. The result is a robust DT that improves situational awareness and supports data-informed decision-making for Chelan PUD's Kaplan turbine operations.

1. INTRODUCTION

With an average machine age exceeding 64 years, the U.S. hydropower fleet faces a pressing need for smart modernization. This modernization is essential for reducing costs and enhancing the reliability and value of the nation's longest-serving renewable energy technology. As hydropower increasingly plays a vital role in maintaining grid reliability and resiliency, operations are becoming more complex and demanding, particularly with the introduction of nonlinear dynamics. The continual expansion of variable renewable energy production, such as solar and wind, further intensifies pressure on the grid. To remain competitive, hydropower technology must integrate the latest advancements in sensors, data management, control systems, analytics, simulation, optimization, and computing capabilities [1].

In this context, digital twins (DTs) emerge as powerful tools that provide a virtual environment for engineers and operators to simulate and optimize performance. A DT is a sophisticated virtual replica or simulator of a physical object, system, or process, mirroring the real-world characteristics, behaviors, and performance of its physical counterpart. Serving as an effective platform for research and development (R&D) and operational management, a well-designed DT facilitates the exploration of best practices for process optimization and real-time monitoring. Creating an effective DT requires meticulous modeling of various components within the hydropower system, including the penstock, turbine, generator, and their interconnections with the broader power grid [2].

As power demand increases, hydropower systems must operate over a broader range, which can induce nonlinear characteristics in generation units. For instance, a Francis hydroturbine exhibits two primary nonlinearities: mechanical torque and water flow [1]. Both are influenced by factors such as water head,

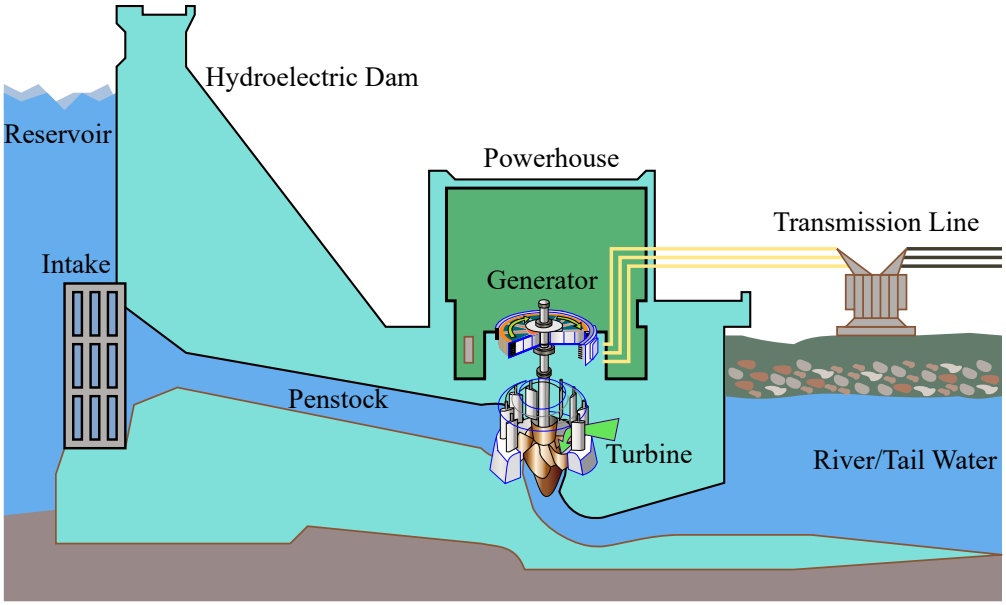

Figure 1. Functional diagram of a hydroelectric system with a turbine. Turbine converts the kinetic and potential energy of the flowing water into rotational mechanical energy. The wicket gates controls the volume and flow rate of water from the reservoir through a penstock to the turbine, which in turn adjusts the turbine's mechanical torque. The shaft system connects the turbine to the generator, transmitting the mechanical torque and rotation. The generator uses the rotational energy transmitted from the shaft to produce electrical output power via electromagnetic induction. [4].

hydroturbine shaft speed, and guide vane opening. Fig. 1 shows a functional diagram of a hydropower generation system, in which the water flows from the reservoir flows a penstock to the hydroturbine, which then drives a synchronous generator to generator electricity. To understand the dynamics of the hydroturbine system, it is essential to estimate these nonlinear functions using real-time operational data obtained from the programmable logic controller in the distributed control system [3]. In this context, neural network modeling may be particularly well-suited for adaptive learning, enabling the effective capture of complex nonlinear dynamics [5]. These advanced algorithms enhance the accuracy and predictive capabilities of DT models by leveraging historical and real-time data. For instance, neural networks analyze data on water inflow, turbine performance, and energy production to identify patterns that forecast future behavior of the hydropower system. By providing valuable insights, this modeling strategy enables operators to anticipate changes, optimize energy production, and make informed decisions, ultimately enhancing operational efficiency and minimizing downtime [6].

2. COMPONENTS OF HYDROPOWER SYSTEMS

The operational system for hydropower generation units is comprised of several modules, which include penstock dynamics, a shaft speed sensor/controller, and a hydraulic servo. Fig. 2 shows a generic structure of a hydropower generation unit, in which the water from the reservoir flows through a penstock (pipe) to the hydroturbine, which then drives a synchronous generator to generate the electricity. Turbine converts the kinetic and potential energy of the flowing water into rotational mechanical and electrical power generation for grid integration is achieved by adjusting the guide vane, an inlet water valve that regulates the flow of water into the hydroturbine chamber. Thus, the guide vane opening serves as the control input, while rotational mechanical energy and generated power are the outputs transmitted to the power grid.

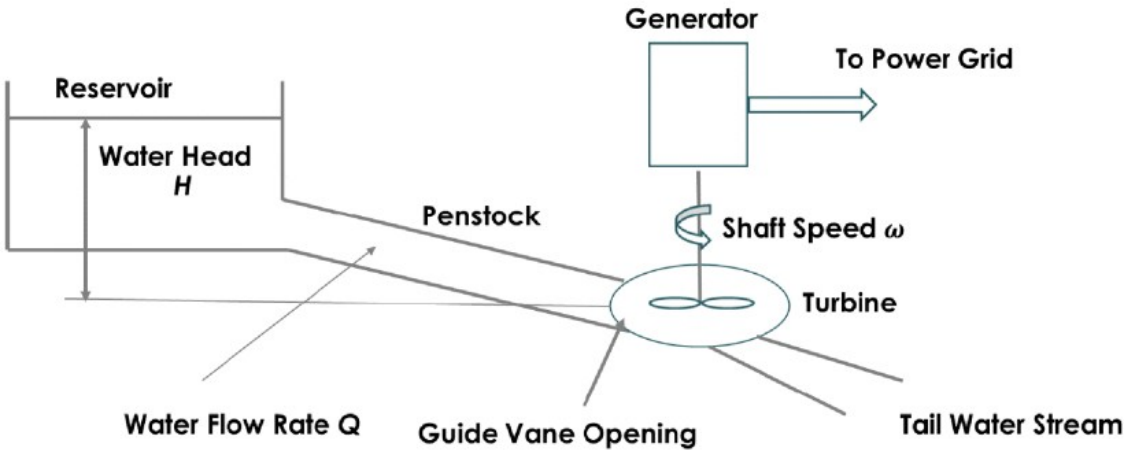

Figure 2. The hydropower system, where the generator is driven by a turbine which converts the kinetic and potential energy of the flowing water into rotational mechanical energy. Shaft whose speed (ω) is adjusted by the opening of a guide vane that controls the water flow from the reservoir through a penstock to the turbine [1].

2.1 RESERVOIR

Acts as a water storage system, controlling flow and providing a supply of water for power generation. The reservoir can be formed by constructing a dam across a river or by utilizing existing natural lakes. The size and capacity of the reservoir are determined based on hydrological studies, ensuring it can store enough water to meet demand fluctuations. The water level in the reservoir affects the potential energy available for generation.

2.2 HYDROELECTRIC DAM

A barrier that impounds water to create the reservoir, controlling its release to optimize electricity production while managing flood risks.

2.3 PENSTOCK

The penstock is a critical component of a hydropower system, serving as a conduit for high-pressure water flow from the reservoir to the turbine. Understanding the dynamics of the penstock is essential for optimizing hydropower performance and ensuring system reliability. When evaluating the penstock dynamics in hydropower systems, depending on the length of pipe and water ahead, considering water elasticity and flow characteristics, is essential.

2.4 TURBINE

Converts the kinetic and potential energy of water into mechanical energy. Common types include Francis, Kaplan, and Pelton turbines, selected based on head conditions.

Kaplan turbines operate in low-head environments, typically ranging from 2 to 30 meters, resulting in lower pressure levels in the penstock and the hydraulic system. At these lower pressures, water behaves more as an incompressible fluid, displaying nonelastic characteristics. The reduced compressibility means that changes in flow do not result in significant variations in water volume or pressure within the penstock.

The outputs of the water flow rate (Q) and turbine torque (M) can be described by the following equations:

$$Q = g(H, \omega, u, \alpha) \tag{1}$$

$$M = f(H, \omega, u, \alpha) \tag{2}$$

where H is the operating water height, ω is the turbine runner rotational, u is the inlet valve opening, and α is the blade angle.

Additionally, g and f are the nonlinear functions for the flow rate and turbine torque, respectively. Assuming the turbine operates at an operating point $O = (\omega_0, H_0, Q_0, u_0, \alpha_0)$ and considering the nonelastic water flow, we can introduce the relative (normalized) incremental values as follows:

$$\begin{aligned} x &= \frac{\omega - \omega_0}{\omega_0}, \quad h = \frac{H - H_0}{H_0}, \quad q = \frac{Q - Q_0}{Q_0}, \\ \Delta u &= \frac{u - u_0}{u_0}, \quad \Delta\alpha = \frac{\alpha - \alpha_0}{\alpha_0}, \end{aligned} \tag{3}$$

where all variables are normalized incremental values: x for shaft speed, h for water head, q for water flow rate, Δu for guide vane opening, and $\Delta\alpha$ for blade angle.

Kaplan turbine has its particularity as blade angle adjustment is critical for optimal efficiency. These turbines operate under a wide range of flow conditions by maintaining optimal blade angles between the water flow and the blade surfaces. Thus, the blade angle, α, is a function of the wicket gate opening, u, and the influence of water net head, H, represented as:

$$\alpha = d(u, H), \tag{4}$$

which is normally approximated by a 5^{th} order polynomial, this leads to the following linearized model:

$$\Delta\alpha = \frac{\partial d}{\partial u}(O)\Delta u \tag{5}$$

2.5 GENERATOR

Transforms mechanical energy from the turbine into electrical energy through electromagnetic induction, essential for power output. Most hydropower plants use synchronous generators, which operate at a constant speed depending on the frequency of the electrical grid. The rotor spins within a magnetic field produced by stator windings, inducing current in the coils.

The dynamic model of a synchronous generator, described by five differential equations in Equation (6) in the d-q reference frame, captures its electromechanical and electromagnetic behavior for transient stability

analysis [**?**].

$$\begin{cases} \frac{d\delta}{dt} = \omega_0 \Delta\omega \\ \frac{d\omega}{dt} = \frac{1}{2M}(T_m - T_e - K_D \Delta\omega) \\ T'_{d0} \frac{dE'_q}{dt} = X_{ad} I_f - E'_q - I_d(X_d - X'_d) \\ T''_{d0} \frac{dE''_q}{dt} = E'_q - E''_q - I_d(X'_d - X'_{d'}) \\ T''_{q0} \frac{dE''_d}{dt} = -E''_d + I_q(X_q - X''_q) \end{cases} \tag{6}$$

In (6), the first term adjusts rotor angle (δ) via speed deviation ($\Delta\omega = \omega - \omega_0$) with ω_0 as synchronous frequency. The second term sets rotor speed (ω) using mechanical torque (T_m), electromagnetic torque (T_e), inertia (M), and damping (K_D). The third term updates q-axis transient voltage (E'_q) with field current (I_f), d-axis current (I_d), reactances (X_{ad}, X_d, X'_d), and time constant (T'_{d0}). The fourth term manages q-axis subtransient voltage (E''_q) with reactance (X''_d) and time constant (T''_{d0}). The fifth term controls d-axis subtransient voltage (E''_d) with q-axis current (I_q), reactances (X_q, X''_q), and time constant (T''_{q0}).

In the given equation, T_m is the mechanical torque from water flow to the turbine, $T_e = P/\omega$ is the load torque, K_D is the generator's damping ratio, and $\Delta\omega = \omega - \omega_0$ is the turbine rotational speed deviation from its nominal value ω_0. Since the unit is grid-connected, $\Delta\omega$ is typically small and hence we can omit it and hence Equation 6 is simplified as:

$$\begin{cases} T'_{d0} \frac{dE'_q}{dt} = X_{ad} I_f - E'_q - I_d(X_d - X'_d) \\ T''_{d0} \frac{dE''_q}{dt} = E'_q - E''_q - I_d(X'_d - X''_d) \\ T''_{q0} \frac{dE''_d}{dt} = -E''_d + I_q(X_q - X''_q) \end{cases} \tag{7}$$

2.6 CONTROL SYSTEM

Manages plant operations, including flow monitoring and turbine adjustments, and encompasses sensors, Programmable logic controller (PLC), and analysis software. Two of the main control systems in the hydropower generation i.e., turbine and synchronous generator systems are valve opening for Guided vane opening (time-variant) (u) and excitation control input for Excitation control input for generator (v). u controls frequency and active power generation while v controls voltage and reactive power.

2.6.1 Excitation Systems

Fig. 3 shows the block diagram of PSLF excitation system based on model ESST5B [7]. Excitation in a synchronous generator fundamentally involves supplying a precisely controlled Direct current (DC) to the rotor's field windings, thereby establishing a fundamental-frequency rotating magnetic field. This field, rotating synchronously with the prime mover, electromagnetically couples with the stationary stator windings, inducing an Electromotive force (EMF) whose magnitude is directly proportional to the field current and rotor speed. An Automatic voltage regulator (AVR) constitutes the core of the control mechanism, continuously sensing the generator's terminal voltage and comparing it to a reference. Any detected voltage deviation generates an error signal, which the AVR processes via sophisticated control algorithms (e.g., PI, lead-lag compensation) to adjust the exciter's output. The exciter, whether a static rectifier, brushless Alternating current (AC) exciter with rotating rectifiers, or a DC exciter, then modulates the DC current to the main generator's field, closing the feedback loop to maintain target terminal voltage and contribute to reactive power control and overall system stability.

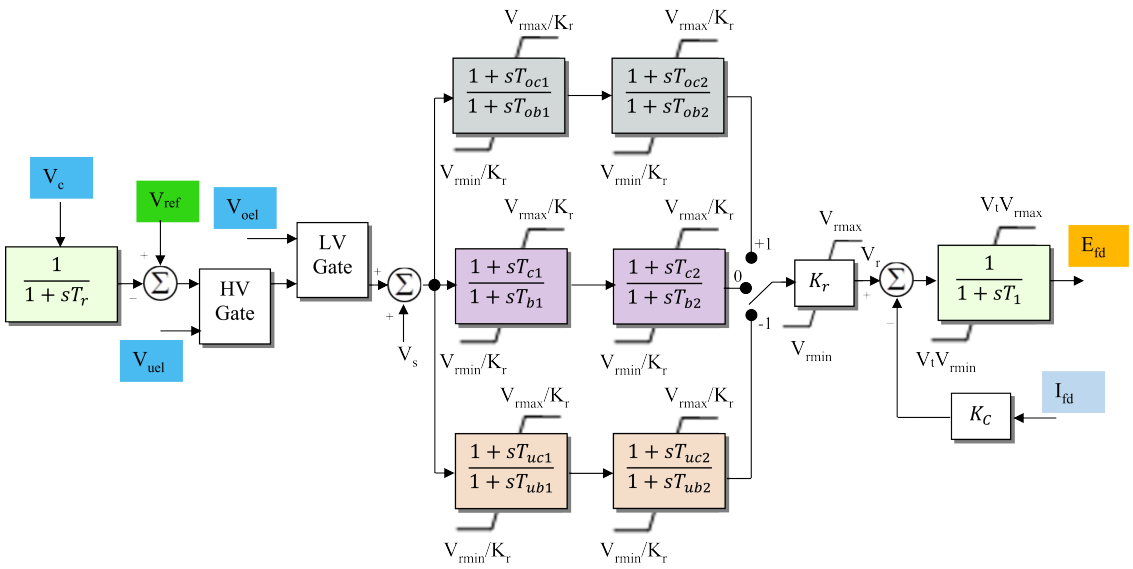

Figure 3. Block diagram of PSLF excitation system model ESST5B [7].

2.6.2 PIDD Controller

Fig. 4 illustrates a sophisticated control system, centered on the Proportional–Integral–Double–Derivative (PIDD) controller, an advanced variant of the standard Proportional–Integral–Derivative (PID). This controller is used by many hydropower systems due to its enhanced transient response and oscillation damping. The frequency control system processes the frequency deviation $\Delta\omega$ to generate a control variable (CV) for the turbine-governor. A conventional PID structure is shown for reference; however, this work employs the PIDD controller, which extends the PID formulation by including an additional filtered second-derivative term to improve damping and transient response. The controller incorporates proportional, integral, derivative, and second-derivative actions implemented using first-order dynamic blocks and filtered derivative paths to avoid noise amplification. Electrical power feedback P_{elec}, auxiliary power input P_{aux}, and coordinated gate feedback (R_{gate}, R_{elec}) are included for operating-point correction and stability. Controller output is limited by saturation blocks defined by $P_{\max}$ and $P_{\min}$, and deadband nonlinearities (db_1) model insensitivity to small frequency deviations. The control variable CV drives the turbine-governor actuator, which includes rate limits, deadbands (db_2), and first-order lags, producing the gate position GV. Hydraulic and mechanical dynamics are represented using the water starting time T_w, turbine gain A_t, and damping D_{turb}, yielding the mechanical power output P_{mech} normalized on the machine MVA base. All model variables and parameters are defined in Appendix A.

2.7 TAILRACE

A channel or pipe for discharging water downstream after generated power passes through the turbine returning to river, helping to maintain the ecological flow of the river.

2.8 ELECTRICAL INFRASTRUCTURE

Comprises transformers, switchgear, and transmission lines, facilitating the integration of generated power into the electrical grid. The electrical infrastructure must comply with standards to ensure safety and reliability, addressing factors such as load flow analysis and short circuit calculations.

2.9 FISH LADDERS/BYPASS SYSTEMS

Facilitate the migration of aquatic life around or past the dam, mitigating ecological impacts.

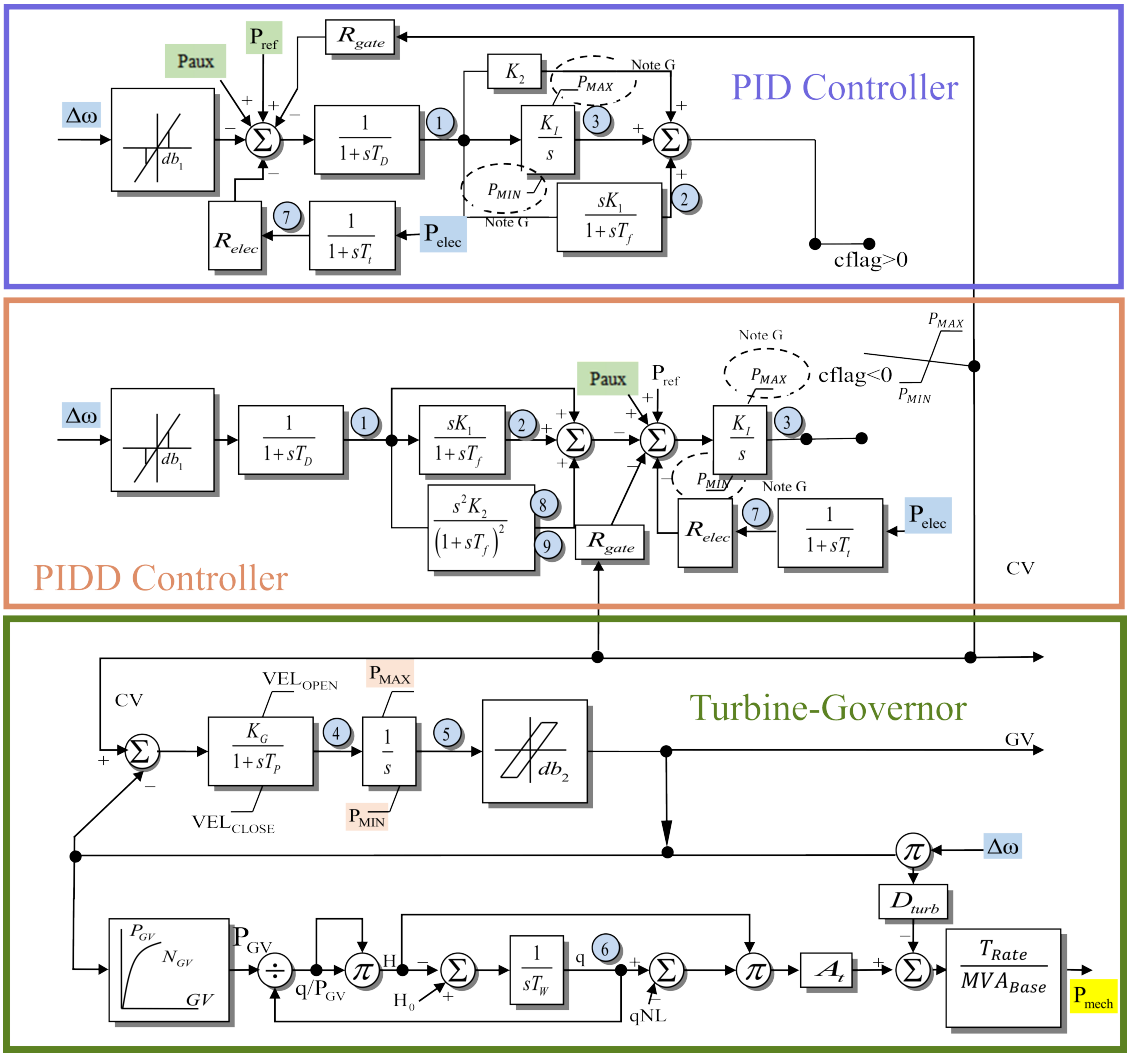

Figure 4. Block diagram of PIDD controller [7].

3. UNDERSTANDING THE DIGITAL TWINS (DT)

DT concept was initially introduced in 2003 and the researches rapid growth in recent years which cover a lot of areas and industry fields. DT is defined as a virtual replica of a physical object, system or process that serves as a digital counterpart. Fig. 5 illustrates the essential components of a DT for hydropower systems—an open platform framework. This begins with real data from a reference hydropower unit/plant, which is processed through a central data processing module. This data feeds into a system of dynamic models, including penstock dynamics, hydro turbine dynamics, generator dynamics, and tail water dynamics, which collectively form the core of the DT operation and control. The processed data and model outputs are then can be interfaced with the user's visualization tools, enabling interaction and analysis. Simultaneously, the DT can also interacts with a power grid module, incorporating different operational load modes and forecasting, to optimize operation and control The DT captures the plant's operations in a dig-

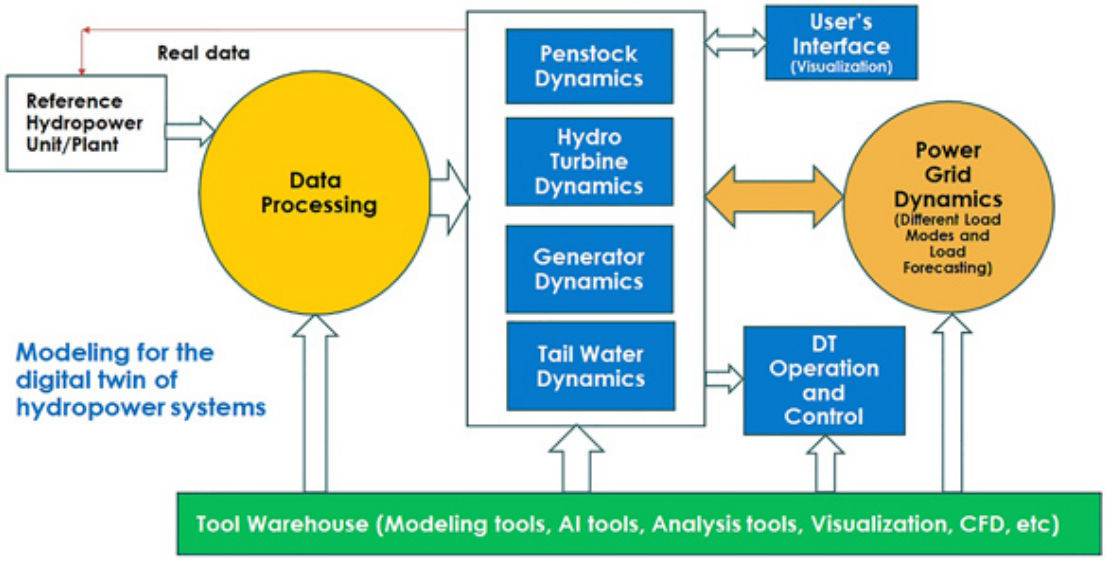

Figure 5. The flow diagram shows the overview of proposed structure for the modeling scope of a DT for hydropower systems. This requires the modeling of the penstock system, the hydro-turbine, the generator and the tail water system and thus motivates the novel hybrid modeling of hydro-turbine dynamics using a neural network [1].

ital format, supporting operational optimization, condition monitoring, and workforce training. In order to develop an effective DT, dynamic modeling of the entire system is crucial, encompassing the penstock, turbine, generator, and power grid connections. To achieve accurate replication of the hydropower system's dynamics, adaptive learning techniques should be employed for online training of the dynamic models, enabling them to reliably mirror real-time behavior to simulation capabilities to enhance operational efficiency, improve maintenance strategies, and ensure system reliability and sustainability.

3.1 TURBINE SYSTEM MODEL

The water system for electricity generation must account for the reservoir, penstock, turbine chamber, and discharge (tail water stream), forming a complex nonlinear hydropower dynamic system. This system requires data-driven modeling along with initial manufacturing data from turbine manufacturers. Utilizing hydropower turbine-generator experimental data allows us to create a systematic model for simulating the hydropower generator system in digital twin development.

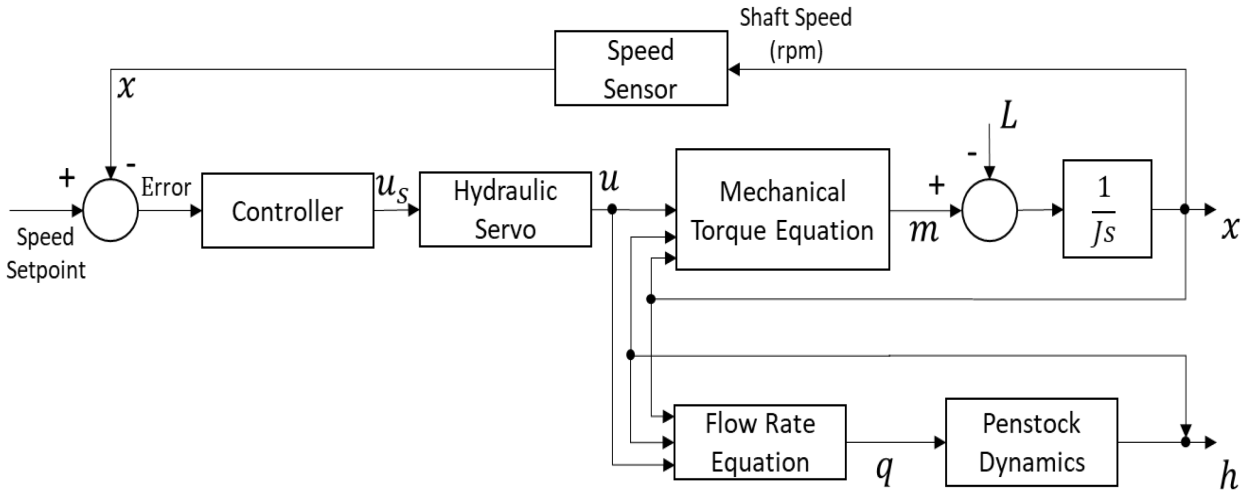

Figure 6. Control flow of the hydropower turbine control system.

3.1.1 Turbine Speed Control System

Fig. 6 illustrates the closed-loop turbine speed control structure, integrating the controller, hydraulic servo, turbine mechanical dynamics, and water conduit dynamics. The controller compares the measured turbine–generator shaft rotational speed x with the speed setpoint to form a control error, which is processed to generate the servo control signal. The hydraulic servo block represents the actuator dynamics that convert the controller output into the guide vane opening, thereby regulating the water flow rate q into the turbine. The turbine mechanical block computes the mechanical torque m produced by the runner as a function of water flow and hydraulic head. The rotor inertia block $1/(Js)$ represents the turbine–generator shaft dynamics, where J is the combined rotational inertia, integrating the net mechanical torque (including the load disturbance L) to produce the shaft speed x. The water conduit (penstock) dynamics block represents the transient relationship between flow rate q and water head h, capturing hydraulic storage and wave effects. The primary system outputs are the shaft rotational speed (frequency) x and the water head h. Through speed feedback, the control loop regulates turbine speed under varying load disturbances during grid-connected operation while mitigating transient fluctuations in water flow and hydraulic head.

3.1.2 Torque and Water Flow Module

Figure 2 illustrates the torque and water flow rate modules for the hydropower turbine during operation. The dynamics of the system indicate that the inputs are the guide vane opening, turbine runner rotational speed, and water head, while the outputs are the turbine torque M and water flow rate Q. The following nonlinear functions are typically defined [1, 3]:

$$Q = g(H, \omega, u, \alpha)$$

$$M = f(H, \omega, u, \alpha)$$

where α represents the blade angle, ω represents the turbine speed (rad/s), related to frequency by $\omega = 2\pi f_0$, with f_0 maintained around 60 Hz for the US system when the hydropower unit is connected to the grid. In Equations (1) and (2), H is the water head, and u is the guide vane opening. The functions g and f are unknown nonlinear functions that must be learned using real-time operational data.

The water system of a Kaplan turbine includes a reservoir, penstock, turbine chamber, and discharge (tail water stream). The outputs of the water flow rate (Q) and turbine torque (M) can be described by the fol-

lowing equations:

$$Q = g(H, \omega, u, \alpha) \tag{8}$$

$$M = f(H, \omega, u, \alpha) \tag{9}$$

where H is the operating water height, ω is the turbine shaft speed, u is the inlet valve opening, and α is the blade angle. Additionally, g and f are the nonlinear functions for the flow rate and turbine torque, respectively. Assuming the turbine operates at an operating point $O = (\omega_0, H_0, Q_0, u_0, \alpha_0)$ and considering the nonelastic water flow, we can introduce the relative (normalized) incremental values as follows:

$$\begin{aligned} x &= \frac{\omega - \omega_0}{\omega_0}, \quad h = \frac{H - H_0}{H_0}, \quad q = \frac{Q - Q_0}{Q_0}, \\ \Delta u &= \frac{u - u_0}{u_0}, \quad \Delta\alpha = \frac{\alpha - \alpha_0}{\alpha_0}, \end{aligned} \tag{10}$$

where all variables are normalized incremental values: x for shaft speed, h for water head, q for discharge water flow rate, Δu for guide vane opening, and $\Delta\alpha$ for blade angle.

Kaplan turbines have a distinctive feature in that blade angle adjustment is critical for achieving optimal efficiency. These turbines operate over a wide range of flow conditions by maintaining an appropriate blade angle relative to the discharge water flow and blade surfaces. Accordingly, the blade angle α is modeled as a function of the wicket gate opening u and the net water head H, expressed as

$$\alpha = d(u, H), \tag{11}$$

which is commonly approximated using a fifth-order polynomial. Linearizing this relationship around an operating point O yields

$$\Delta\alpha = \left.\frac{\partial d}{\partial u}\right|_O \Delta u. \tag{12}$$

By incorporating this linearized relationship between $\Delta\alpha$ and Δu, the expressions for turbine mechanical torque and flow rate can be reduced to a six-parameter linear model. Specifically, the mechanical torque is given by

$$\begin{aligned} m &= \bar{e}_x x + \left(\bar{e}_u + \bar{e}_\alpha \left.\frac{\partial d}{\partial u}\right|_O\right)\Delta u + \bar{e}_h h \\ &= e_x x + e_u \Delta u + e_h h, \end{aligned} \tag{13}$$

where x denotes the turbine–generator shaft speed and h denotes the water head.

Similarly, the turbine flow rate can be expressed as

$$\begin{aligned} q &= \bar{e}_{qx} x + \left(\bar{e}_{qu} + \bar{e}_{q\alpha} \left.\frac{\partial d}{\partial u}\right|_O\right)\Delta u + \bar{e}_{qh} h \\ &= e_{qx} x + e_{qu} \Delta u + e_{qh} h. \end{aligned} \tag{14}$$

The coefficients e_x, e_u, e_h, e_{qx}, e_{qu}, and e_{qh} are obtained by linearizing the original nonlinear turbine torque and flow equations about the operating point O. These coefficients depend on partial derivatives of the nonlinear functions $f(\cdot)$ (mechanical torque) and $g(\cdot)$ (flow rate), evaluated at O, and are defined as

$$e_x = \bar{e}_x, \quad e_u = \bar{e}_u + \bar{e}_\alpha \left.\frac{\partial d}{\partial u}\right|_O, \quad e_h = \bar{e}_h,$$

$$e_{qx} = \bar{e}_{qx}, \quad e_{qu} = \bar{e}_{qu} + \bar{e}_{q\alpha} \left.\frac{\partial d}{\partial u}\right|_O, \quad e_{qh} = \bar{e}_{qh}.$$

As a result, in any cases the objective of learning is to use the measured turbine runner rotational speed, the water pressure, and the guide vane opening to estimate the mechanical torque dynamics $f(x, h, u)$ and the water flow dynamics $g(x, h, u)$. The turbine model uses past values of power and control input to predict the current output power. The neural network learns the nonlinear function $\hat{P}(k) = g_\phi(\cdot)$ as follows:

$$\hat{P}(k) = g_{\phi_1}\left(P(k-1), P(k-2), u(k-1), u(k-2)\right) + g_{\phi_2}\left(u(k-1), u(k-2)\right) \tag{15}$$

3.2 GENERATOR SYSTEM MODEL

The following generator model is modeled using NN.

$$\begin{cases} T'_{d0}\frac{dE'_q}{dt} = X_{ad}I_f - E'_q - I_d(X_d - X'_d) \\ T''_{d0}\frac{dE''_q}{dt} = E'_q - E''_q - I_d(X'_d - X''_d) \\ T''_{q0}\frac{dE''_d}{dt} = -E''_d + I_q(X_q - X''_q) \end{cases} \tag{16}$$

In the above equations, E'_q and E''_q denote the transient and subtransient internal electromotive forces (emfs) on the q-axis, respectively, while E''_d denotes the subtransient internal emf on the d-axis. The variables I_d and I_q represent the stator current components along the direct (d) and quadrature (q) axes, respectively, expressed in the rotor reference frame. The parameter I_f denotes the field current, and X_{ad} is the mutual (armature–field) reactance relating field current to the internal emf. The parameters X_d and X_q are the synchronous reactances on the d- and q-axes, while X'_d and X''_d are the transient and subtransient d-axis reactances, and X''_q is the subtransient q-axis reactance. The time constants T'_{d0} and T''_{d0} are the open-circuit transient and subtransient time constants on the d-axis, respectively, and T''_{q0} is the open-circuit subtransient time constant on the q-axis. These differential equations describe the electromagnetic dynamics of a synchronous machine in the dq reference frame, capturing the transient and subtransient behavior of the rotor circuits.

The generator model is more complex and estimates $\hat{Q}(k)$ and $\hat{V}_t(k)$ using a combination of recent and delayed values, expressed as a sum of two neural network outputs:

$$\begin{aligned} \hat{Q}(k), \hat{V}_t(k) = {} & f_{\theta_1}(P(k-1), V_f(k), V_f(k-1), V_f(k-2), \\ & V_t(k-1), V_t(k-2), V_t(k-3), Q(k-1), Q(k-2), Q(k-3), I_f(k)) \\ & + f_{\theta_2}(P(k-1), V_f(k), V_f(k-1), V_f(k-2), I_f(k)) \end{aligned} \tag{17}$$

$$\begin{aligned} \Delta\hat{Q}(k) = {} & f_{\theta_3}(P(k-1), V_f(k), V_f(k-1), V_f(k-2), \\ & V_t(k-1), V_t(k-2), V_t(k-3), Q(k-1), Q(k-2), Q(k-3), I_f(k)) \end{aligned} \tag{18}$$

$$\tilde{Q}(k) = Q(k) - \Delta\hat{Q}(k) \tag{19}$$

$$\text{Loss} = \text{MSE}((\hat{Q}(k), \hat{V}_t(k)), \ (\tilde{Q}(k), V_t(k))) \tag{20}$$

The model then incorporates an iterative update using the mean square error and the difference $\Delta\hat{Q}(k)$ as $\Delta\hat{Q}(k)$ is computed based on the mean square error to adjust the output iteratively through the feedback loop and added to $\hat{Q}(k)$ to refine the estimate (i.e., $\hat{Q}(k) = \hat{Q}(k) + \Delta\hat{Q}(k)$).

where:

- $V_f(k)$: Field voltage,
- $V_t(k)$: Terminal voltage,
- $Q(k)$: Reactive power,
- $I_f(k)$: Field current,
- $\theta_1, \theta_2, \theta_3$: Parameters of the respective neural networks.

4. DATA REQUIREMENTS

Instead of constructing physical modeling for simulating the turbine and generator system, this study simplifies the hydropower system and solved through the neural network modeling. Thus, it is important to obtain accurate real-world hydropower data as much as possible for the neural network model's training and validation to predict and analyze system behavior. In specific, this project conducts neural network modeling with the data collected from the Kaplan turbine Unit 3 generator owned and operated by Chelan County Public Utilities District.

4.1 DATA SOURCES AND SIGNALS

The dataset comprises measurements recorded by the plant's supervisory control and data acquisition (SCADA) system and other process instrumentation.

Table 1. Signals and descriptions (Unit C03)

Signal	Description
C03_GOV_WG_POS	Turbine guided vane (governor) position
C03_EXC_FLD_CURR	Exciter field current
C03_EXC_FLD_VOLT	Exciter field voltage
C03_GEN_PHZ_A_VOLT	Generator terminal voltage (Phase A)
C03_GEN_MW_OUT	Generator active power output (MW)
C03_GEN_MVAR_OUT	Generator reactive power output (MVAR)
C03_MW_SETPOINT	Generator power control setpoint
C03_SCRL_PIEZ_2_PRES	Scroll-case piezo #2 pressure
C03_SCRL_PIEZ_3_PRES	Scroll-case piezo #3 pressure
C03_SCRL_PIEZ_6_PRES	Scroll-case piezo #6 pressure
C03_UNIT_SPD_RPM	Unit rotatioal speed (RPM)

These signals capture the system's dynamic response to control actions and external disturbances. Fig. 7, 8, and 9 shows the data format that is required to train the NN model.

4.2 DATA PROCESSING

To prepare the data for modeling, several preprocessing steps were applied:

- **Downsampling:** Reducing the data frequency by selecting every *n*th sample to balance temporal resolution and computational efficiency.
- **Truncation:** Limiting the dataset to a maximum number of samples to ensure manageable dataset size.
- **Normalization and scaling:** Centering variables around nominal operating points and scaling by suitable factors to improve training stability and convergence.

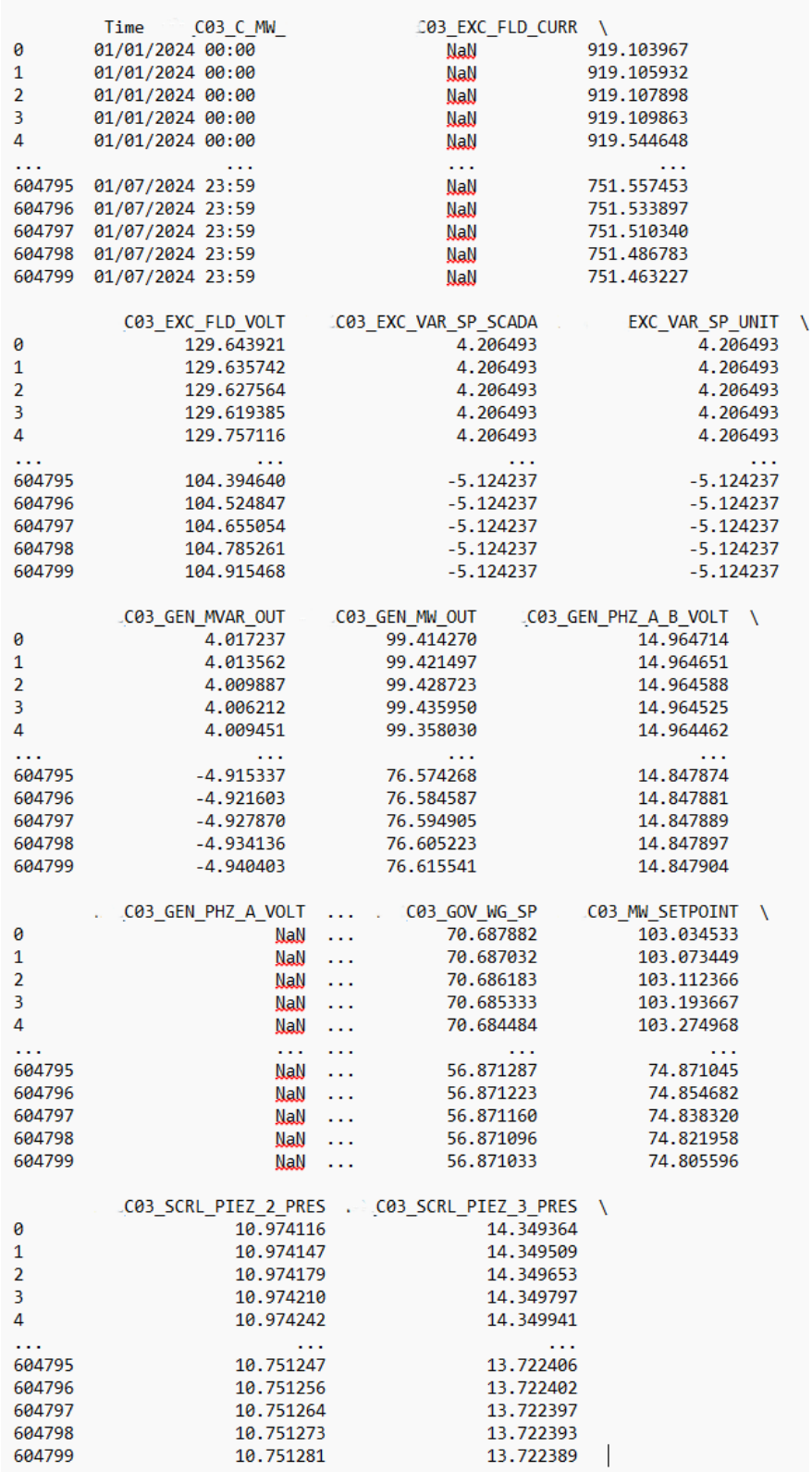

	Time	C03_C_MW_	C03_EXC_FLD_CURR	\
0	01/01/2024 00:00		NaN	919.103967
1	01/01/2024 00:00		NaN	919.105932
2	01/01/2024 00:00		NaN	919.107898
3	01/01/2024 00:00		NaN	919.109863
4	01/01/2024 00:00		NaN	919.544648
...	...		...	...
604795	01/07/2024 23:59		NaN	751.557453
604796	01/07/2024 23:59		NaN	751.533897
604797	01/07/2024 23:59		NaN	751.510340
604798	01/07/2024 23:59		NaN	751.486783
604799	01/07/2024 23:59		NaN	751.463227

	C03_EXC_FLD_VOLT	C03_EXC_VAR_SP_SCADA	EXC_VAR_SP_UNIT	\
0	129.643921	4.206493	4.206493	
1	129.635742	4.206493	4.206493	
2	129.627564	4.206493	4.206493	
3	129.619385	4.206493	4.206493	
4	129.757116	4.206493	4.206493	
...	...	...	...	
604795	104.394640	-5.124237	-5.124237	
604796	104.524847	-5.124237	-5.124237	
604797	104.655054	-5.124237	-5.124237	
604798	104.785261	-5.124237	-5.124237	
604799	104.915468	-5.124237	-5.124237	

	C03_GEN_MVAR_OUT	C03_GEN_MW_OUT	C03_GEN_PHZ_A_B_VOLT	\
0	4.017237	99.414270	14.964714	
1	4.013562	99.421497	14.964651	
2	4.009887	99.428723	14.964588	
3	4.006212	99.435950	14.964525	
4	4.009451	99.358030	14.964462	
...	...	...	...	
604795	-4.915337	76.574268	14.847874	
604796	-4.921603	76.584587	14.847881	
604797	-4.927870	76.594905	14.847889	
604798	-4.934136	76.605223	14.847897	
604799	-4.940403	76.615541	14.847904	

	C03_GEN_PHZ_A_VOLT	...	C03_GOV_WG_SP	C03_MW_SETPOINT	\
0	NaN	...	70.687882	103.034533	
1	NaN	...	70.687032	103.073449	
2	NaN	...	70.686183	103.112366	
3	NaN	...	70.685333	103.193667	
4	NaN	...	70.684484	103.274968	
...	...	...	...	...	
604795	NaN	...	56.871287	74.871045	
604796	NaN	...	56.871223	74.854682	
604797	NaN	...	56.871160	74.838320	
604798	NaN	...	56.871096	74.821958	
604799	NaN	...	56.871033	74.805596	

	C03_SCRL_PIEZ_2_PRES	C03_SCRL_PIEZ_3_PRES	\
0	10.974116	14.349364	
1	10.974147	14.349509	
2	10.974179	14.349653	
3	10.974210	14.349797	
4	10.974242	14.349941	
...	...	...	
604795	10.751247	13.722406	
604796	10.751256	13.722402	
604797	10.751264	13.722397	
604798	10.751273	13.722393	
604799	10.751281	13.722389	

Figure 7. Input data sample collected from unit 3 of Chelan County PUD.

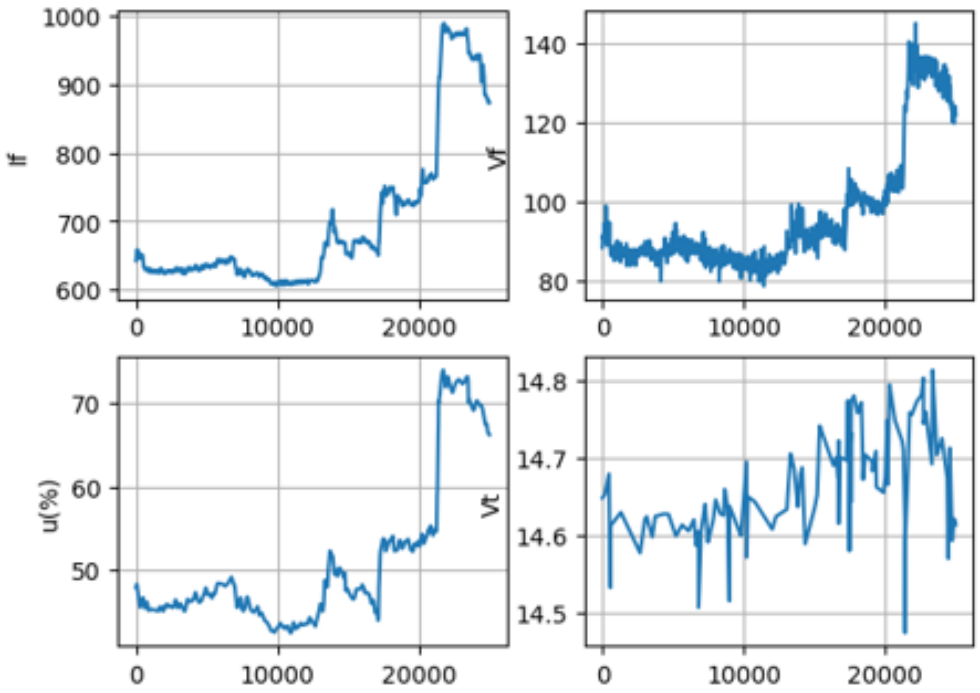

Figure 8. Input data sample: Field current, voltage, gate opening, and terminal voltage.

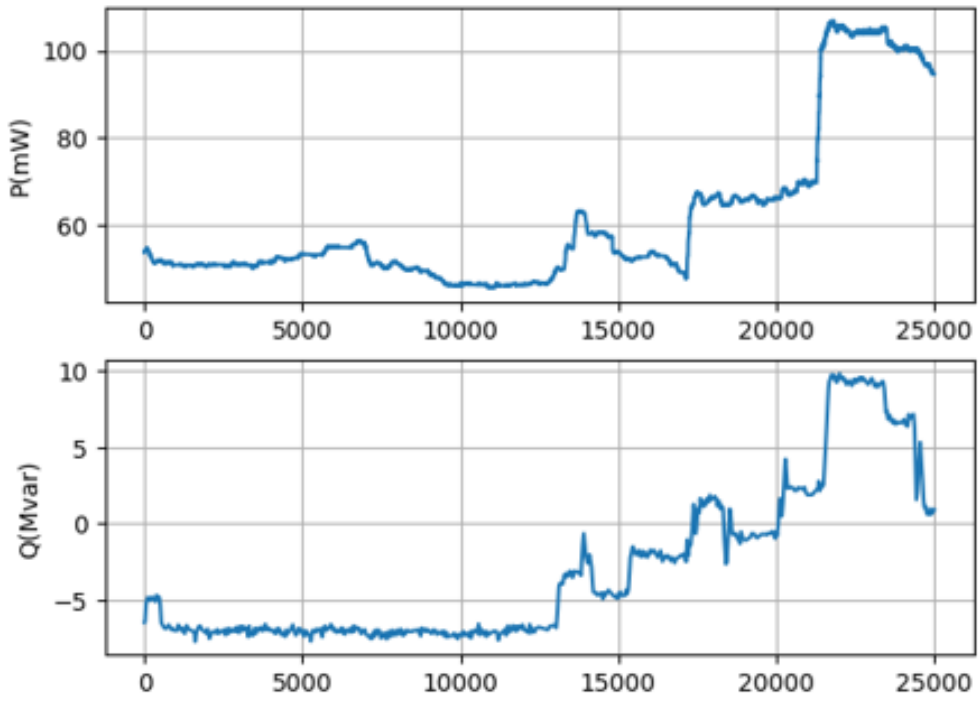

Figure 9. Input data sample: Active and reactive power.

4.3 DATASET PREPARATION

The dataset was divided into training and testing subsets, typically using a test ratio (e.g., 20%) to reserve a portion of the data for model validation. Time-series lag features were created to capture temporal dependencies, using historical values of input and output variables (e.g., values at $t-1$, $t-2$, etc.). This approach helps the model learn dynamic relationships and improve prediction accuracy.

4.4 DATASET SUMMARY

The processed datasets were combined to create comprehensive training and testing datasets. A suitable batch size was chosen for model training to balance convergence speed with available computational resources. This structured data preparation ensures that the model can capture the underlying dynamics and produce reliable predictions during deployment.

5. MODELING TECHNIQUES

As power demand increases, hydropower systems must operate over a broader range, which can induce nonlinear characteristics in generation units and hence, it is essential to estimate these nonlinear functions using real-time operational data obtained from the programmable logic controller in the distributed control system. In this context, neural network modeling may be particularly well-suited for adaptive learning, enabling the effective capture of complex nonlinear dynamics. These advanced algorithms enhance the accuracy and predictive capabilities of DT models by leveraging historical and real-time data.

5.1 TYPES OF MODELING

Various modeling techniques can be applied to turbine-generator dynamics, each suited to different scenarios. This section explores these types, with a focus on neural network models and the rationale for selecting the Multi-Layer Perceptron (MLP) in the current implementation.

5.1.1 Overview of Modeling Types

- **Physical Modeling**:
  - Based on differential equations from physical laws, e.g., the swing equation: $M\frac{d^2\delta}{dt^2} = P_m - P_e - D\frac{d\delta}{dt}$, where δ is the rotor angle, P_m is mechanical power, P_e is electrical power, M is inertia, and D is damping.
  - Advantages: High accuracy for known systems, interpretable.
  - Challenges: Requires detailed system data, computationally intensive.
- **State-Space Modeling**:
  - Uses a set of first-order differential equations: $\dot{x} = Ax + Bu$, $y = Cx + Du$, where x is the state vector, u is the input vector, and y is the output vector.
  - The matrix A is the state matrix, which characterizes the internal system dynamics and the coupling among state variables.
  - The matrix B is the input matrix, which maps the external inputs to the state dynamics.
  - The matrix C is the output matrix, which maps the system states to the measured or controlled outputs.
  - The matrix D is the feedthrough (or direct transmission) matrix, which represents the instantaneous effect of the inputs on the outputs.
  - Advantages: Suitable for control design and well suited for multi-input multi-output (MIMO) systems.
  - Challenges: Assumes linearity and requires accurate state estimation.
- **Reinforcement Learning (RL)**:
  - Employs agents to learn optimal policies via trial and error, optimizing a reward (e.g., maximizing power while stabilizing voltage).
  - Advantages: Adapts to changes, no explicit model needed.
  - Challenges: Requires extensive data, computationally expensive.
- **Neural Network Modeling**:
  - Utilizes data-driven approaches to learn complex, non-linear relationships.
  - Discussed in detail below due to its use in the current implementation.

5.1.2 Neural Network Models

Within the neural network paradigm, several architectures can model turbine-generator dynamics:

- **Recurrent Neural Network (RNN)**:
  - Includes memory through recurrent connections, suitable for time-series data like turbine-generator outputs.
  - Strengths: Captures temporal dependencies directly.
  - Limitations: Prone to vanishing gradients, less effective for long sequences.
- **Long Short-Term Memory (LSTM)**:
  - An advanced RNN variant with memory cells, ideal for long-term dependencies in power system data.
  - Strengths: Better gradient flow, handles delayed inputs well.
  - Limitations: Higher computational cost, complex training.
- **Convolutional Neural Network (CNN)**:
  - Uses convolutional layers to extract spatial features, adaptable for time-series with 1D convolutions.
  - Strengths: Efficient feature extraction, parallelizable.
  - Limitations: Less suited for non-spatial turbine-generator data.
- **Multi-Layer Perceptron (MLP)**:
  - A feedforward network with fully connected layers, used here with architectures like turbine NN, generator NN, and Q refining NN model.
  - Strengths: Effective for static mappings, handles non-linearities with historical data.
  - Limitations: Limited in capturing temporal dynamics without additional preprocessing.

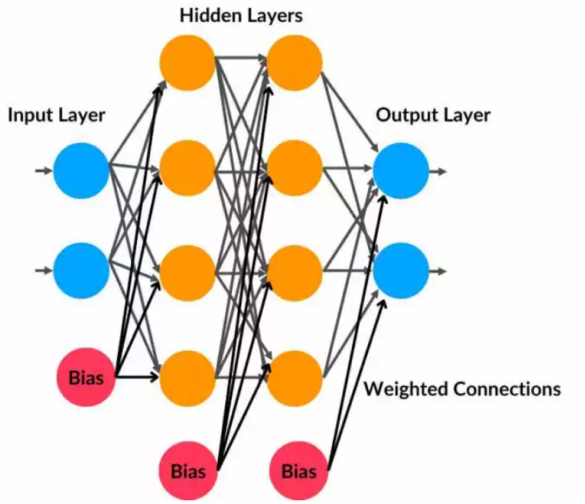

Figure 10. Architecture of MLP.

This research utilizes a MLP, a foundational feedforward neural network characterized by its layered architecture (input, hidden, output) of fully connected neurons. As shown in Fig. 10, an MLP's structure is defined by its Layers: an input layer receives data, one or more hidden layers perform complex transformations, and an output layer delivers the final prediction. Within these layers, neurons utilize Activation Functions (like ReLU, ELU, or Sigmoid) to introduce non-linearity, enabling the network to learn intricate relationships. The network undergoes Learning by iteratively adjusting its internal parameters (weights and biases). This process often involves minimizing a Mean Squared Error (MSE) loss function, where the network's predictions are compared to actual targets, and the difference is minimized through optimization algorithm. During operation, MLPs make predictions via forward propagation, where input data flows through the layers. Learning occurs through backpropagation, an iterative process that computes error gradients from predicted versus actual outputs, which an optimizer then uses to adjust the network's internal weights and biases, minimizing prediction errors.

5.2 FACTORS INFLUENCING NEURAL NETWORK DESIGN

The design should consider the following system-specific and data-specific attributes:

- **System Type:** Static (algebraic) vs. dynamic (time-dependent).
- **Order of Dynamics:** Number of significant past time steps influencing current behavior.
- **System Nonlinearity:** Degree of deviation from linear models.
- **Data Availability:** Volume, resolution, and quality of historical input/output data.
- **Computational Constraints:** Real-time vs. offline applications.

5.3 SELECTING NEURAL NETWORK TYPE

- **Feedforward Neural Network (FNN) / MLP:**
  - Suitable for static systems or when using pre-structured past input/output as features.
  - Requires manual inclusion of lag terms.
- **Recurrent Neural Network (RNN):**
  - Captures dynamic, time-sequential behaviors.
  - Better suited for systems where temporal memory is important (e.g., generator voltage and current response).
- **Long Short-Term Memory (LSTM):**
  - A type of RNN ideal for systems with long-term dependencies.
  - Recommended when system response depends on long sequences of past events.
- **NARX Networks (Nonlinear AutoRegressive with eXogenous inputs):**
  - Designed for dynamic systems using delayed inputs and outputs explicitly.
  - Well-suited when delays are known and bounded.

5.4 MODEL ORDER SELECTION

Model order defines how many past time steps (lags) are included as inputs:

- Use **system identification** or autocorrelation/partial correlation plots to determine relevant lags.
- For turbines and generators, orders between 2–5 are typical, depending on response time and sampling rate.
- Rule of thumb: include sufficient lags to cover at least 2–3 dominant time constants of the system.

5.5 NETWORK DEPTH AND WIDTH

- **Number of Layers (Depth):**
  - 1–2 hidden layers are sufficient for most physical system modeling.
  - Use 3+ layers only for highly nonlinear or composite systems.
- **Number of Neurons per Layer (Width):**
  - Start with 2–4 times the number of input features in the first layer.
  - Reduce neurons in deeper layers (pyramid structure) to avoid overfitting.
- Use grid search or Bayesian optimization to fine-tune architecture.

5.6 ACTIVATION FUNCTION SELECTIONS

- **ReLU (Rectified Linear Unit):** Preferred in deep networks to mitigate vanishing gradients.
- **tanh:** Useful for modeling both positive and negative values (e.g., voltage deviations).
- **sigmoid:** Rarely used due to saturation and slow convergence.
- **Linear:** Use in output layer for regression tasks.

5.7 REGULARIZATION AND OPTIMIZATION

- **Dropout:** Randomly disable neurons during training to prevent overfitting.
- **L2 regularization (weight decay):** Penalizes large weights.
- **Batch normalization:** Stabilizes learning.
- **Optimizer:** Use Adam or RMSProp for efficient convergence.
- **Learning rate schedule:** Reduce learning rate gradually during training.

5.8 EVALUATION AND VALIDATION

- Use **Mean Square Error (MSE)** or **Mean Absolute Error (MAE)** for regression.
- Perform **time-series cross-validation** or rolling window validation.
- Visualize predicted vs. actual outputs to verify accuracy over time.

Aspect	Recommendation
NN Type	FNN/MLP for static; RNN/LSTM/NARX for dynamic systems
Order	2–5 lags, based on system time constants
Hidden Layers	1–3 (more for high nonlinearity)
Neurons/Layer	2–4× number of inputs, then reduce in deeper layers
Activations	ReLU/tanh (hidden), Linear (output)
Optimizer	Adam or RMSProp
Regularization	Dropout, L2
Evaluation	MSE, MAE, time-series validation

5.9 CHOOSING THE RIGHT NEURAL NETWORK MODEL

The selection of the MLP for this turbine-generator modeling task was guided by several considerations:

- **Data Characteristics**: Availability of preprocessed historical data (e.g., P_{last}, $V_{t,\text{last}}$, Q_{last}) with up to three time delays allowed the MLP to learn static mappings effectively after proper input normalization.
- **Computational Efficiency**: MLPs require less computational resources compared to RNNs or LSTMs, making them suitable for offline simulation and pre-trained model evaluation under real-time constraints.
- **Model Simplicity**: The dual-network structure in MLPNet_{Gene} and single-network $\text{Net}_{Q_{diff}}$ provided enough flexibility to handle 11 inputs without the complexity of recurrent architectures, since delays were included manually.
- **Training Data Availability**: The dataset and pre-trained checkpoints were optimized for MLP training, supporting this architecture choice.
- **How to Choose**: The process involved:
  - Framing the task as static regression with delayed inputs.
  - Validating performance of MLP versus alternatives (e.g., LSTM) on holdout data.
  - Accounting for deployment constraints such as inference speed and memory usage.
- **Rationale**: MLP was selected for its balance of accuracy, simplicity, and speed, leveraging delayed inputs to capture temporal effects. $\text{Net}_{Q_{diff}}$ added an iterative refinement mechanism akin to feedback control.

This approach ensures robust predictions while remaining computationally practical for the current implementation.

6. DESIGN AND JUSTIFICATION OF NN ARCHITECTURE FOR TURBINE–GENERATOR MODELING

6.1 OVERVIEW

In dynamic modeling of power systems, neural networks (NNs) learn nonlinear maps from lagged signals. We adopt discrete-time models:

$$\hat{P}(k) = g_{\phi_1}(P(k-1), P(k-2), u(k-1),\ u(k-2)) + g_{\phi_2}(u(k-1),\ u(k-2)) \quad \text{(Turbine model)} \tag{21}$$

$$\begin{bmatrix} \hat{Q}(k) \\ \hat{V}_t(k) \end{bmatrix} = f_{\theta_1}(\underbrace{P(k-1),\ V_f(k),\ V_f(k-1),\ V_f(k-2),\ V_t(k-1),\ V_t(k-2),\ V_t(k-3),\ Q(k-1),\ Q(k-2),\ Q(k-3),\ I_f(k)}_{\text{11 features}}) + f_{\theta_2}(\underbrace{P(k-1),\ Q(k-1),\ Q(k-2),\ Q(k-3),\ I_f(k)}_{\text{5 features}}), \quad \text{(Generator dual-branch)} \tag{22}$$

and, when needed, a single-branch model for reactive power:

$$\hat{Q}(k) = h_\psi(P(k-1),\ V_f(k),\ V_f(k-1),\ V_f(k-2),\ V_t(k-1),\ V_t(k-2),\ V_t(k-3),\ Q(k-1),\ Q(k-2),\ Q(k-3),\ I_f(k)). \tag{23}$$

In Eqs. (21)–(23), k denotes the discrete-time index. $\hat{P}(k)$ is the predicted mechanical power output of the turbine at time k, and $P(k)$ is the measured mechanical power. The variable $u(k)$ denotes the turbine control input (e.g., guide vane or gate command). Functions $g_{\phi_1}(\cdot)$ and $g_{\phi_2}(\cdot)$ are neural network mappings parameterized by weights ϕ_1 and ϕ_2, respectively, representing the main turbine dynamics and an auxiliary correction branch.

In the generator models, $\hat{Q}(k)$ and $\hat{V}_t(k)$ denote the predicted reactive power and terminal voltage magnitude, respectively, while $Q(k)$ and $V_t(k)$ denote their measured values. The variable $V_f(k)$ is the generator field voltage, and $I_f(k)$ is the field current. The functions $f_{\theta_1}(\cdot)$ and $f_{\theta_2}(\cdot)$ are neural networks parameterized by θ_1 and θ_2, forming a dual-branch architecture in which f_{θ_1} captures the dominant nonlinear generator dynamics and f_{θ_2} provides an auxiliary correction based on a reduced feature set.

Equation (23) defines a single-branch neural network model $h_\psi(\cdot)$, parameterized by ψ, used when only reactive power prediction is required. All lagged terms (e.g., $P(k-1)$, $Q(k-2)$, $V_t(k-3)$) represent past samples used to capture system dynamics in discrete time. The symbols ϕ_1, ϕ_2, θ_1, θ_2, and ψ collectively denote the trainable parameters of the corresponding neural networks.

6.2 GENERAL NEURAL NETWORK DESIGN CONSIDERATIONS

6.3 TURBINE NEURAL NETWORK (`TURBINE_NET`)

Inputs/Outputs

$$\hat{P}(k)\& = g_{\phi_1}(P(k-1), P(k-2), u(k-1),\ u(k-2)) + g_{\phi_2}(u(k-1),\ u(k-2))$$

Table 2. Guiding Principles for NN Architecture Selection

Aspect	Design Implication
System Order	Include sufficient time-lagged variables in inputs
System Type	Generator: nonlinear & coupled; Turbine: lower-order with strong input effect
Function Complexity	1 hidden layer (128) with ELU + BN balances capacity & stability
Data Availability	Avoid overparameterization; use dropout where branches are high-capacity
Real-Time Constraints	Prefer shallow/efficient networks; evaluate in `float64` when needed

Architecture (PyTorch)

```
# net1: full 4-D input, with dropout
nn.Sequential(
    nn.Dropout(p=0.5),
    nn.Linear(4, 128),
    nn.BatchNorm1d(128),
    nn.ELU(),
    nn.Linear(128, 1)
)

# net2: 2-D subset input: [u(k-1), u(k-2)]
nn.Sequential(
    nn.Linear(2, 128),
    nn.BatchNorm1d(128),
    nn.ELU(),
    nn.Linear(128, 1)
)

# forward: output = net1(x) + net2(x[:, [2,3]])
```

Design Justification

- **Two branches (additive):** Mirrors the decomposition in (21) with a full-context branch and a focused input-only branch capturing direct gate effects.
- **Dropout (0.5) in net1:** Regularizes the higher-capacity full-input branch.
- **Hidden Units (128) + ELU + BN:** Stable gradients, good expressivity for mild turbine nonlinearities.
- **Precision:** `self.double()` enables `float64` inference when long rollouts are used.

6.4 GENERATOR NEURAL NETWORK (`NET_Q_DIFF`)

Inputs/Outputs

The generator model is more complex and estimates $\hat{Q}(k)$ and $\hat{V}_t(k)$ using a combination of recent and delayed values, expressed as a sum of two neural network outputs:

Design Justification

- **Inputs (11):** Deeper memory across V_t and Q plus present V_f, P, and I_f captures coupled generator dynamics.
- **Shallow, single branch:** Improves training stability for $\hat{Q}$ without overfitting.
- **Precision:** `self.double()` for numerically stable long-horizon evaluation.

6.5 GENERATOR DUAL-BRANCH NEURAL NETWORK (`MLPNET_GENE`)

Inputs/Outputs

The generator model is more complex and estimates $\hat{Q}(k)$ and $\hat{V}_t(k)$ using a combination of recent and delayed values, expressed as a sum of two neural network outputs:

Architecture (PyTorch)

```
# net1: full 11-D input
nn.Sequential(
    nn.Dropout(p=0.0),
    nn.Linear(11, 128),
    nn.BatchNorm1d(128),
    nn.ELU(),
    nn.Linear(128, 2)   # two outputs
)

# net2: 5-D subset [P(k-1), Q(k-1), Q(k-2), Q(k-3), I_f(k)]
nn.Sequential(
    nn.Linear(5, 128),
    nn.BatchNorm1d(128),
    nn.ELU(),
    nn.Linear(128, 2)   # two outputs
)

# forward: output = net1(z) + net2(z[:, [0,7,8,9,10]])
```

$$\begin{aligned}\hat{Q}(k), \hat{V}_t(k) = f_{\theta_1}(&P(k-1), V_f(k), V_f(k-1), V_f(k-2),\\ &V_t(k-1), V_t(k-2), V_t(k-3), Q(k-1), Q(k-2), Q(k-3), I_f(k))\\ &+ f_{\theta_2}(P(k-1), V_f(k), V_f(k-1), V_f(k-2), I_f(k))\end{aligned} \tag{24}$$

$$\begin{aligned}\Delta\hat{Q}(k) = f_{\theta_3}(&P(k-1), V_f(k), V_f(k-1), V_f(k-2),\\ &V_t(k-1), V_t(k-2), V_t(k-3), Q(k-1), Q(k-2), Q(k-3), I_f(k))\end{aligned} \tag{25}$$

$$\tilde{Q}(k) = Q(k) - \Delta\hat{Q}(k) \tag{26}$$

Design Justification

- **Two branches (additive):** Implements the decomposition in (22); the subset branch isolates the strongest explanatory subset $\{P(k-1), Q\text{-lags}, I_f(k)\}$.
- **Hidden Units (128) + ELU + BN:** Captures nonlinear cross-terms while keeping training stable.
- **No dropout in net1 (p=0.0):** Retains full information; overall capacity is moderated by BN and the additive split.
- **Precision:** `self.double()` supports stable evaluation with tightly coupled electrical states.

6.6 SUMMARY OF ARCHITECTURES

Model (Class)	Target Outputs	Input Dim.	Special Notes
`turbine_Net`	$\hat{P}(k)$	4	Dual-branch; net1 dropout 0.5; net2 uses $[u(k-1), u(k-2)]$
`Net_Q_diff`	$\hat{Q}(k)$	11	Single-branch; stable baseline for Q
`MLPNet_Gene`	$[\hat{Q}(k),\ \hat{V}_t(k)]$	11 + 5	Dual-branch; subset $[0, 7, 8, 9, 10] = \{P-1, Q\text{-lags}, I_f\}$

Table 3. Summary of neural network architectures used in turbine–generator modeling.

7. CASE STUDIES: CHELAN COUNTY PUBLIC UTILITY DISTRICT

We model the turbine–generator as three coupled neural components that mirror the physics while remaining lightweight for fast rollouts. Each component is a compact MLP with the pattern

$$\text{Linear} \rightarrow \text{BatchNorm1d} \rightarrow \text{ELU} \rightarrow \text{Linear}$$

using 128 hidden units. The `speed` and `generator` networks are evaluated in double precision to improve long-horizon numerical stability.

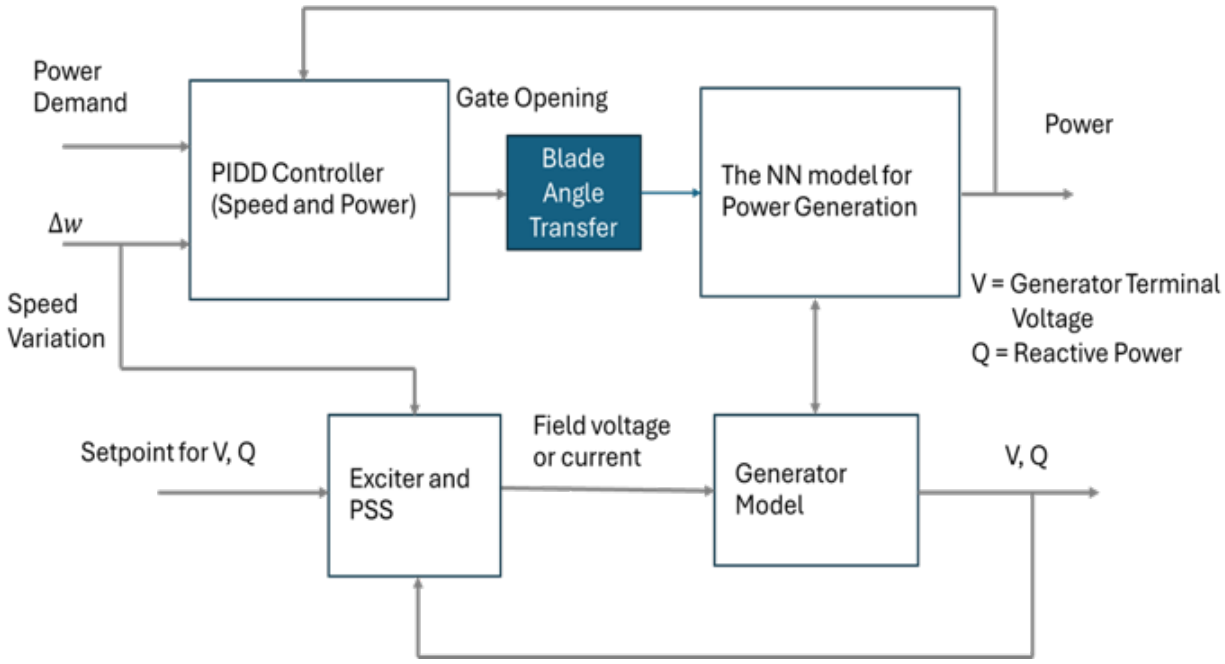

Figure 11. Neural network model structure for rocky reach unit.

The hydropower unit control system, as depicted in Figure 11, is a closed-loop system designed for power and voltage regulation. To develop its digital twin for a Kaplan unit, the system is decomposed into the following functional blocks:

- **Speed/Power Control PIDD:** Primary controller that generates the gate position command u (and, when available, coordinates runner-blade pitch). It regulates active power and speed.
- **NN# Turbine (Power Dynamics):** Learns the turbine's active-power evolution from recent power and gate-history.
- **NN# Generator/Electrical:** Maps the operating point (power history, exciter signals, voltage and reactive-power memory) to terminal electrical quantities. A dedicated corrective branch refines reactive power.
- **Physical System Feedback:** Fixed elements (e.g., an RL path and $\frac{1+T_1 s}{1+T_2 s}$) capturing measurement/actuator dynamics.

Each dynamic component is approximated by compact MLPs (PyTorch) with one hidden layer of 128 units (`BatchNorm1d` + `ELU`); models run in `float64` where long-horizon stability is required.

7.1 NEURAL NETWORK MODEL ARCHITECTURES

7.1.0.1 Turbine (dual-branch) — `turbine_Net`.

$$\hat{P}(k) \;=\; g_{\phi_1}(P(k-1),\, P(k-2),\, u(k-1),\, u(k-2)) \;+\; g_{\phi_2}(u(k-1),\, u(k-2)).$$

Implementation: `net1` takes the full 4-D input with dropout 0.5; `net2` takes the 2-D subset $[u(k-1), u(k-2)]$; outputs are summed. This isolates the strong direct gate influence while preserving full context.

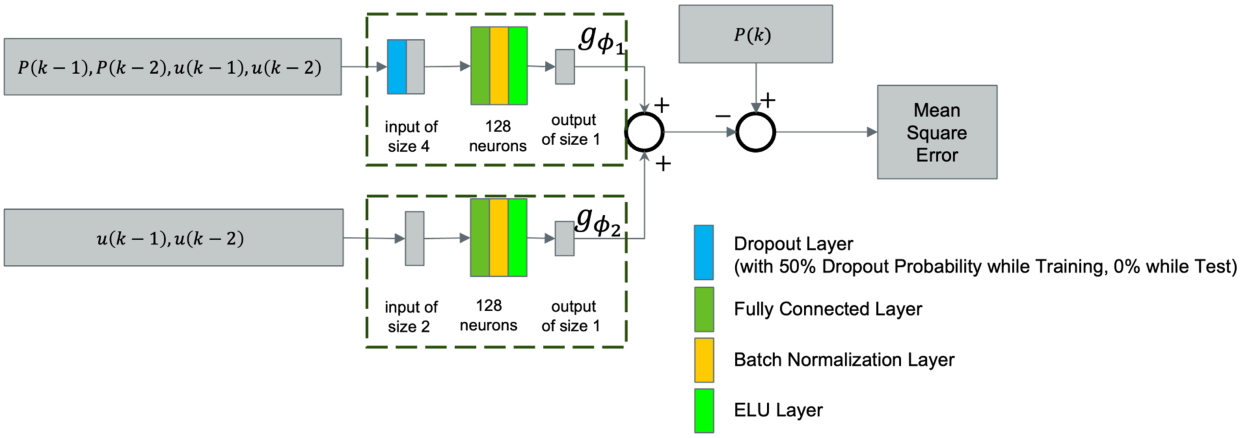

Figure 12. Kaplan turbine neural network model structure for rocky reach unit.

7.1.0.2 Generator (dual-branch) — `MLPNet_Gene`.

$$\begin{bmatrix} \hat{Q}(k) \\ \hat{V}_t(k) \end{bmatrix} \;=\; f_{\theta_1}\Big(\underbrace{P(k-1), V_f(k), V_f(k-1), V_f(k-2), V_t(k-1), V_t(k-2), V_t(k-3), Q(k-1), Q(k-2), Q(k-3), I_f(k)}_{\text{11 features}}\Big)$$
$$+\; f_{\theta_2}\Big(\underbrace{P(k-1), Q(k-1), Q(k-2), Q(k-3), I_f(k)}_{\text{5 features}}\Big).$$

Implementation: `net1` (11-D) and `net2` (5-D) each output two channels; their outputs are summed to yield $[\hat{Q}, \hat{V}_t]$.

7.1.0.3 Reactive-power correction (single-branch) — `Net_Q_diff`.

$$\Delta\hat{Q}(k) \;=\; f_{\theta_3}(P(k-1), V_f(k), V_f(k-1), V_f(k-2), V_t(k-1), V_t(k-2), V_t(k-3), Q(k-1), Q(k-2), Q(k-3), I_f(k)),$$
$$\tilde{Q}(k) \;=\; \hat{Q}(k) \;-\; \Delta\hat{Q}(k).$$

Use: $\Delta\hat{Q}$ compensates residual bias/drift in $\hat{Q}$; $\tilde{Q}$ is the corrected reactive-power estimate.

7.2 TRAINING AND VALIDATION (CONCEPTUAL)

- **Data acquisition:** Operational data covering varying head/flow and exciter regimes; signals include u, P, Q, V_t, V_f (with lags), and I_f.
- **Model training:** Supervised learning with MSE losses per target; Adam optimizer; input normalization; dropout (turbine `net1`) mitigates overfit.
- **Validation:** Hold-out periods; report MAE/RMSE for P, Q, V_t; check long-horizon bias (especially Q) before/after $\Delta\hat{Q}$ correction.

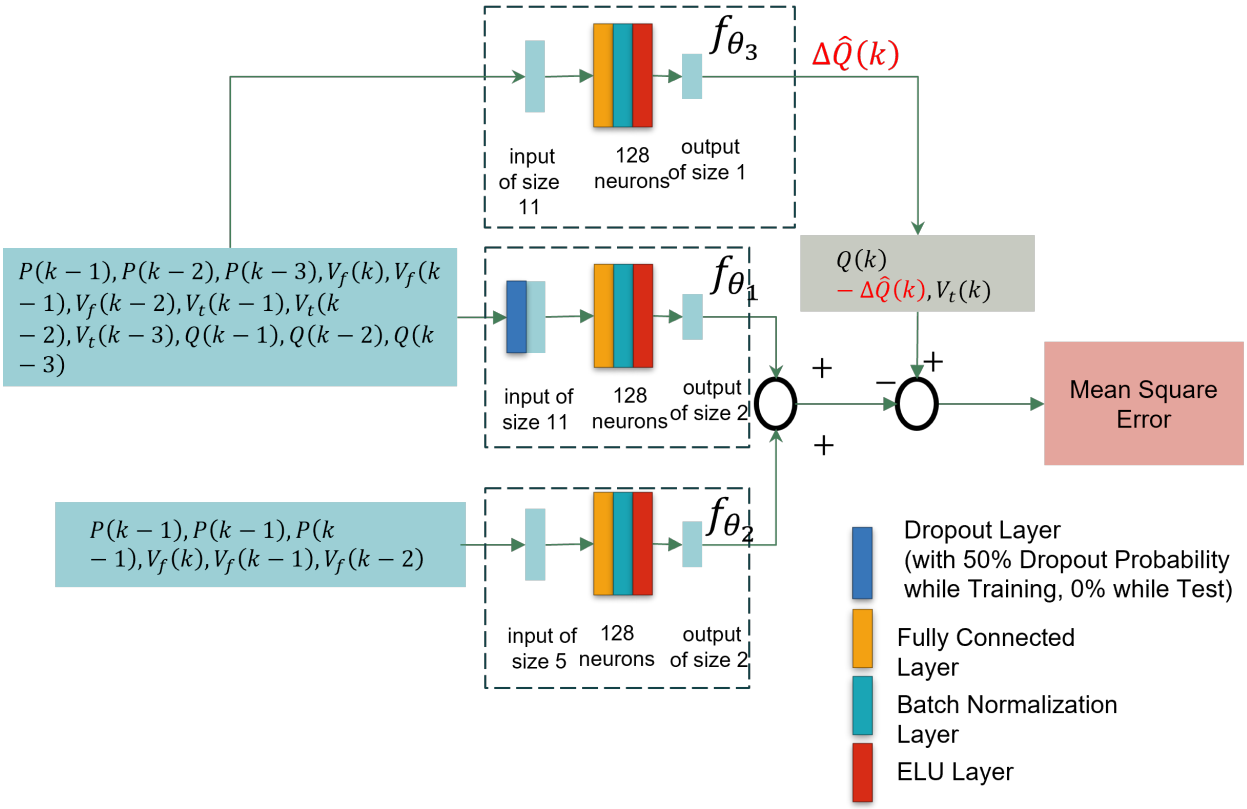

Figure 13. Generator neural network model structure for rocky reach unit.

7.3 DIGITAL TWIN SIMULATION LOOP

7.3.0.1 Initialization.

Use measured histories to warm-start lags for P, Q, V_t, V_f (and I_f as available).

7.3.0.2 Sequential prediction at time t.

1. **Turbine (power):** Compute $\hat{P}(k)$ from $\{P(k-1), P(k-2), u(k-1), u(k-2)\}$ via `turbine_Net`.
2. **Generator (terminal quantities):** Build the 11-D and 5-D inputs from $P(k-1)$, V_f (0–2), V_t (1–3), Q (1–3), and $I_f(k)$; compute $[\hat{Q}(k), \hat{V}_t(k)]$ via `MLPNet_Gene`.
3. **Reactive-power correction (optional):** Compute $\Delta\hat{Q}(k)$ via `Net_Q_diff` and set $\tilde{Q}(k) = \hat{Q}(k) - \Delta\hat{Q}(k)$.

7.3.0.3 Feedback and state update.

- **Errors:** Compare $\hat{P}(k)$ (and, if used for control, $\tilde{Q}(k)$ or $\hat{V}_t(k)$) to their setpoints to form error signals for the external PIDD.
- **Memory update:** Roll lags for P, Q, V_t, V_f to supply $\{\cdot(k-1), \cdot(k-2), \cdot(k-3)\}$ at the next step.

This Kaplan-focused, dual-branch design captures the strong direct gate effects on power while leveraging exciter and electrical-memory features for terminal quantities. The reactive-power correction further reduces bias, improving fidelity for operations and studies at Rocky Reach. Fig. 14 shows the close loop DT response and is compared to the real data from unit 3 of Chelan County PUD.

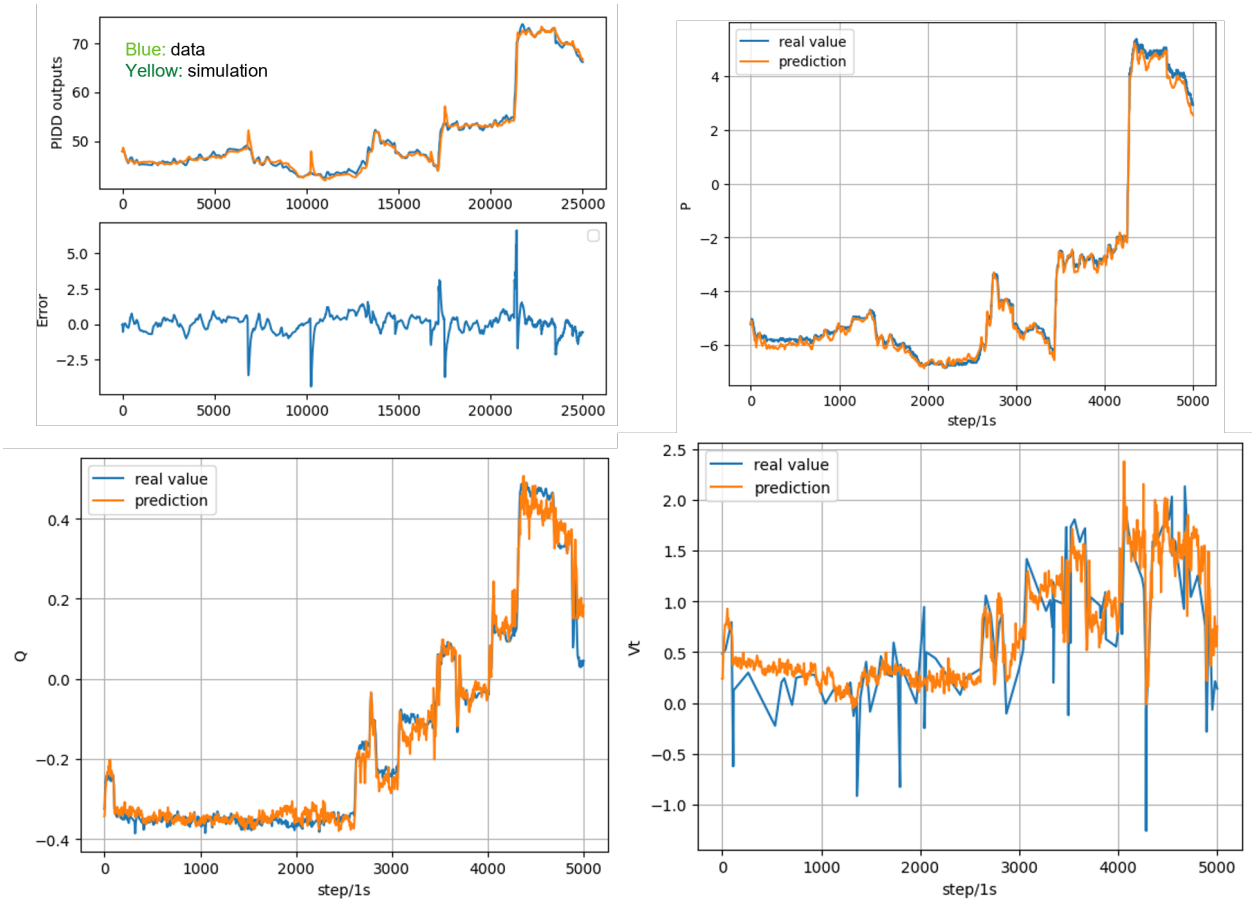

Figure 14. Closeloop response from NN models.

8. CONCLUSIONS

The development and implementation of digital twins for hydropower systems represent a significant advancement in the management and optimization of renewable energy resources. This user manual has provided a comprehensive, step-by-step framework for creating and utilizing digital twins, with a particular focus on leveraging data-driven modeling techniques such as neural networks. By accurately capturing the nonlinear dynamics of hydropower generation units, digital twins enable operators to monitor, predict, and optimize system performance in real time.

This work demonstrates that a compact, dual-branch neural architecture can serve as an accurate and operationally useful digital twin for a Kaplan unit. By decomposing turbine power into a full-context branch and a focused gate-history branch, and by modeling terminal electrical quantities with a paired full/sparse generator network plus a reactive-power correction head, the twin captures key nonlinearities arising from coordinated wicket-gate and runner-blade action, changing head/flow, and exciter dynamics. Trained on operational data, the model reproduces active power, voltage, and reactive power with high fidelity across typical operating ranges.

From an operations standpoint, the Kaplan twin provides fast what-if analysis, disturbance playback, and controller tuning in a risk-free environment. It supports setpoint tracking studies, ramp-rate compliance checks, and voltage/reactive support planning under variable renewable integration. Going forward, adding explicit blade-pitch measurements (when available), broadening data coverage across the gate–blade operating map and seasonal head conditions, and incorporating physics-informed constraints (e.g., cavitation margins, efficiency envelopes) will further improve robustness.

REFERENCES

[1] H. Wang, Z. Yin, and Z.-P. Jiang, “Real-time hybrid modeling of Francis hydroturbine dynamics via a neural controlled differential equation approach," *IEEE Access*, vol. 11, pp. 139133–139146, 2023.

[2] H. Wang, O. Ahmed, K. DeSomber, C. Sasthav, P.-T. Storli, O. Dahlhaug, H. I. Skjelbred, and I. Vilberg, “Adaptive Hybrid 1D Modeling for Digital Twin of Hydropower Systems," Oak Ridge National Laboratory (ORNL), Oak Ridge, TN (United States), Tech. Rep., 2023.

[3] H. Wang, S. Subedi and W. Jia, “Dynamic Modeling of a Kaplan Hydroturbine Using Optimal Parametric Tuning and Real Plant Operational Data." *Dynamics*, 5(2), 2025.

[4] T. Tomia (Original by Tennessee Valley Authority), “Hydroelectric Dam Diagram,” Wikimedia Commons, 30 Dec. 2007. [Online]. Available: https://commons.wikimedia.org/wiki/File:Hydroelectric_dam.svg.

[5] H. Wang and S. Ou, “Structured Neural Network Modeling for Developing Digital Twins Models of Hydropower Generation Units," in *2024 IEEE 19th Conference on Industrial Electronics and Applications (ICIEA)*, 2024, pp. 1–6.

[6] Z. Yin, H. Wang, and Z.-P. Jiang, “Parameter Estimation of Synchronous Generator Using Neural Controlled Differential Equations," in *2024 IEEE 18th International Conference on Control & Automation (ICCA)*, 2024, pp. 332–339.

[7] PowerWorld Corporation, “ESST5B Excitation System Model Description,” Technical Documentation, 2025.

9. APPENDIX A

Table 4. ESST5B Exciter Model Parameters

Parameter	Description
Tr	Filter Time Constant
Kr	Regulator Gain
T1	Firing Circuit Time Constant
Kc	Rectifier Regulation Factor
Vrmax	Maximum Regulator Output
Vrmin	Minimum Regulator Output
Tc1	Regulator Lead Time Constant
Tb1	Regulator Lag Time Constant
Tc2	Regulator Lead Time Constant
Tb2	Regulator Lag Time Constant
Toc1	OEL Lead Time Constant
Tob1	OEL Lag Time Constant
Toc2	OEL Lead Time Constant
Tob2	OEL Lag Time Constant
Tuc1	UEL Lead Time Constant
Tub1	UEL Lag Time Constant
Tuc2	UEL Lead Time Constant
Tub2	UEL Lag Time Constant

10. APPENDIX B

Table 5. HYG3 Governor Model Parameters

Parameter	Description
MWCap	Turbine MW Rating
Pmax	Maximum Gate Opening
Pmin	Minimum Gate Opening
Cflag	Governor Control Flag
Rgate	Steady State Droop for Governor Output Feedback
Relec	Steady State Droop for Electrical Power Feedback
Td	Input Filter Time Constant
Tf	Washout Time Constant
Tp	Gate Servo Time Constant
Velop	Maximum Gate Opening Velocity
Velcl	Maximum Gate Closing Velocity
K1	Derivative Gain
K2	Double Derivative Gain
Ki	Integral Gain
Kg	Gate Servo Gain
Tt	Power Feedback Time Constant
Db1	Intentional Dead-Band Width
Eps	Intentional Dead-Band Hysteresis
Db2	Unintentional Dead-Band
Tw	Water Inertia Time Constant
At	Turbine Gain
Dturb	Turbine Damping Factor
qnl	No-Load Turbine Flow at Nominal Head
H0	Turbine Nominal Head
Gv1	Nonlinear Gain Point 1
Pgv1	Nonlinear Gain Point 1
Gv2	Nonlinear Gain Point 2
Pgv2	Nonlinear Gain Point 2
Gv3	Nonlinear Gain Point 3
Pgv3	Nonlinear Gain Point 3
Gv4	Nonlinear Gain Point 4
Pgv4	Nonlinear Gain Point 4
Gv5	Nonlinear Gain Point 5
Pgv5	Nonlinear Gain Point 5
Gv6	Nonlinear Gain Point 6
Pgv6	Nonlinear Gain Point 6